UCRL--98732

TI89 009902

COMBINED MICROSTRUCTURE X-RAY OPTICS

Troy W. Barbee, Jr.

This paper was prepared for submittal to Review of Scientific Instruments in connection with the 3rd International Conference on Synchrotron Radiation Instrumentation: SRI-88, Tsukuba, Japan, August 29, September 2, 1988.

February 1989

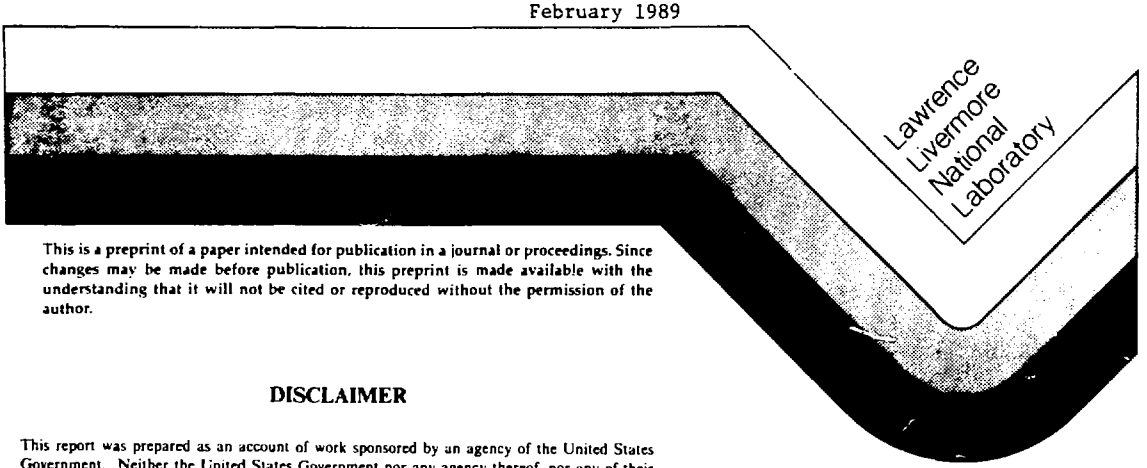

DISCLAIMER

COMBINED MICROSTRUCTURE X-RAY OPTICS

Troy W. Barbee, Jr.

Lawrence Livermore National Laboratory
Livermore CA 94550, USA

ABSTRACT

Multilayers are man-made microstructres which vary in depth and are now of sufficient quality to be used as x-ray, soft x-ray and extreme ultraviolet optics. Gratings are man-made in plane microstructures which have been used as optic elements for most of this century. Joining of these two optical microstructures to form combined microstructure optical elements has the potential for greatly enhancing both the throughput and the resolution attainable in these spectral ranges. The characteristics of these new optic elements will be presented and compared to experiment with emphasis on the unique properties of these combined microstructures. These results reported are general in nature and not limited to the soft x-ray or extreme ultraviolet spectral domains and also apply to neutrons.

INTRODUCTION

Multilayer structures, such as interference filters and reflection or anti-reflection coatings were developed (1) over 50 years ago for the infared, visible, and ultraviolet spectral regions. However, multilayer structures with sufficient quality for advanced optical applications in the x-ray (XR, E>4000eV), soft x-ray (SXR, 100eV< E < 4000eV) and extreme ultraviolet (EUV, 12eV < E < 100eV) have only become available (2,3,4) during the past decade. This capability now provides us with the challenge to design now optical elements that can focus, disperse, or otherwise manipulate XR's, SXR's and EUV light.

In this paper the properties of multilayer diffraction gratings are considered. Diffraction gratings, which are in plane microstructures, were developed in the early 1900's and are a standard dispersive element used in moderate to high resolution applications. The in plane scale of diffraction gratings ranges from approximately 300 to 5000nm. This is to be contrasted with the in depth microstructural scale typical of multilayers which ranges from 1.0 to 40 nm. The convolution of the properties of these two periodic structures results in optic devices which are both unique and technologically useful. Of particular interest is the potential for very high resolution--high efficiency optics operating at near normal incidence in the SXR and EUV domains.

A short description of the multilayer grating structures reported on in this paper and the experimental techniques used are

presented first. A simple analytical model of the properties of multilayer gratings is then presented, and their unique features enumerated. Experimental results are then given, and compared to the analysis presented, the use of multilayer gratings in the determination of the optical constants of materials in the XR, SXR, and EUV being demonstrated. Experimental results for multilayer grating efficiency and resolution are then presented. A simple two element monochromator is described and application of a multilayer-multilayer grating set of dispersion elements to the measurement of the absorption cross sections demonstrated. It is then shown that multilayer gratings act as x-ray prisms. The potential for blaze gratings and true laminar gratings, and the implications as to attainable resolution and monochromator design is then discussed.

EXPERIMENTAL PROCEDURES

The multilayer gratings studied in the work reported here were produced by sputter deposition (2,3) of multilayers onto prepared grating substrates. The grating substrates were fabricated (4) by anisotropic etching of (110) orientation single crystal silicon and had a period of 2 μm with 1 μm bars. The etched grooves were deep (> 3μm) and rough so that these multilayer gratings were simple amplitude gratings. Multilayers of period d_0 composed of two materials (A and B) containing N layer pairs have been synthesized onto grating substrates and characterized.

These multilayer diffraction grating structures have been

studied at the Stanford Synchrotron Radiation Laboratory on Beamline III-4 (5), a differentially pumped line gathering 0.6 mr of synchrotron light from a bending magnet. The beamline consists of the bending magnet source, a gold coated collimating mirror giving a high energy cutoff of approximately 3.5 keV, a differential pumping system allowing the experimental chamber to be a pressures up to 10^{-5} torr, a single or double multilayer dispersion element monochromator, and adjustable slit scanning detectors. Facilities for introduction of incident spectrum limiting filters, transmission absorption cross-section samples, and transmission gratings for calibration of the light transmitted by the multilayer optics are also available.

The monochromator is shown schematically in Figure 1. Multilayer 1 is mounted on a large externally driven rotary table with its front surface on the center of rotation at point 0. In the two dispersion element mode multilayer 2 is mounted on the same rotating table and has three additional degrees of motion. First, it is mounted on an x-y stage giving linear motions normal and parallel to its front surface. These motions allow the diffracted beam from multilayer 1 to be followed as θ is varied from 2° to 80° while maintaining, h, the spacing of the incident and exit beams constant. The third motion is rocking of multilayer 2 about axis A for alignment and rocking curve measurements. A second rotating table allows a detector to be mounted in the monochromator chamber. When multilayer 2 is moved out of the beam diffracted by multilayer 1, this detector is used to scan the dispersed beam or to measure the rocking curve of multilayer 1 as θ is varied. Another detector is

mounted in a chamber approximately 1150 mm from the grating. This detector may be both vertically and horizontally scanned and was typically slitted to a 100 μm.

Three types of experiments have been performed with multilayer gratings. First, the grating is mounted in the multilayer 1 position. Data is taken by scanning the grating in θ (grating scan) with the detector fixed or by scanning the detector while holding θ constant (detector scan). Second, a two dispersion element configuration is used with the grating mounted in the multilayer 2 position. Again, either the grating is rocked with a fixed detector or the detector is scanned with a fixed grating. Third, an absorption sample is introduced into the incident beam, characteristic absorption edges providing energy and resolution calibration.

MULTILAYER DIFFRACTION GRATINGS

Multilayer diffraction gratings are combined microstructure devices as shown in the schematic cross-section in Figure 2. The in-plane or grating structure has a period d_g and consists of flat topped bars of width $d_g/2$. This structure is a simple laminar amplitude grating as light is only diffracted from the tops of the grating bars by the multilayers. The multilayer structure is periodic in depth with a period d_0 as shown. Light incident a grazing angle θ and is diffracted by the multilayer at an exit angle θ in zeroeth order. Interference of light diffracted by the multilayer on each grating bar results in intensity maxima (grating dispersed multilayer diffracted light) at angles $m\phi$ relative to zeroeth order

where m (=±1, ±2, ±3 --) are the grating orders. In the following the relationship between the dispersion angle ϕ, the structural parameters d_g and d_0, the angle of incidence θ, and the composition of the multilayer is developed.

Two approaches to a simple analytic description of the characteristics of multilayer gratings are of interest. The first is by direct analogy with a simple symmetric transmission grating (1) of period d_g. Light incident at angle θ onto such a grating is dispersed as if the grating has a period of d_g Sin θ (i.e. the grating period is foreshortened). The grating equation then becomes:

$$\text{Sin } \Phi_m = m\lambda/d_g \text{ Sin } \theta \qquad (1)$$

where Φ_m is the dispersion angle of the m^{th} order relative to the zeroeth order beam, and λ the wavelength of the dispersed light If we now assume this grating is a reflecting multilayer grating (as shown in Figure 2), the wavelength dispersed is determined by the angle of incidence θ and the multilayer period d_0 through Bragg's equation (6)

$$n\lambda = 2d^*\text{Sin}\theta \qquad (2)$$

where d^* is the refraction corrected multilayer period (to be discussed later) and n the order of Bragg reflection. Solving Eq. 2 for $\lambda/\text{Sin}\theta$ and substituting into Eq. 1 yields

$$\text{Sin } \Phi_m = 2md^*/nd_g \qquad (3)$$

This equation states that the dispersion angle Φ_m of the m^{th} grating order is constant being independent of θ, the angle of incidence or the wavelength of the dispersed light, as a result of the convolution of the properties of these two periodic structures. This is a unique property making possible conceptual new XR, SXR and EUV instrumentation.

The response of a multilayer diffraction grating may also be derived in more complete form using the scalar grating equation (7)

$$m\lambda = d_g (\text{Sin } \alpha + \text{Sin } \beta) \qquad (4)$$

where α and β are angles relative to the grating normal as defined in Figure 2. Noting that Sin β = Sin $(-\alpha+m\phi)$ = Sin $m\phi$ Cos α – Cos $m\phi$ Sin α Equation 4 can be rewritten as

$$m\lambda/d_g = \text{Sin } \phi_m + \text{Cot } \theta \ (1- \text{Cos } \phi_m) \qquad (5)$$

Again one can substitute for λ/Sin θ from Bragg's equation (Eq. 2) giving

$$2md^*/nd_g = \text{Sin } \phi_m + \text{Cos } \theta \ [1 - \text{Cos } \phi_m] \qquad (6)$$

The second term on the right of Eq. 6 is small except at the highest orders (m > 15) of light diffracted by very high dispersion gratings so that this equation reduces to Eq. 3 under most experimental

conditions. The complete form of Equations 3 and 6 include the refraction correction to the multilayer period.

By the use of Snell's Law it may be shown (6) that the refraction corrected period d^* is given by

$$d^* = d_0[\, 1 - (2\,\bar{\delta} - \bar{\delta}^2) \,/\, \mathrm{Sin}^2\theta \,]^{1/2} \qquad (7)$$

where d_0 is the geometric multilayer period and δ is the spatially averaged scattering component of the multilayer refractive index. δ is given by

$$\bar{\delta} = \delta_A \,(t_A / d_0) + \delta_B \,(t_B / d_0) \qquad (8)$$

where t_A, t_B and δ_A, δ_B are the thicknesses and scattering components of the refractive of layers A and B respectively.

The most useful form of Equations 3 and 6 is gained by assuming the second term on the right of Eq. 6 is negligible and substituting d^* of Eq. 8:

$$\mathrm{Sin}\,\phi = \mathrm{Sin}\,\phi_0\,[\, 1 - (2\bar{\delta} - \bar{\delta}^2)/\,\mathrm{Sin}^2\,\theta \,]^{1/2} \qquad (9)$$

where $\mathrm{Sin}\,\phi_0 = 2md_0/nd_g$. The refraction correction term is nearly constant over broad spectral ranges away from characteristic absorption edges of materials A and B of the multilayer. Therefore, ϕ_m is nearly constant as concluded earlier and wholly determined by the multilayer period (d_0), the grating period (d_g) and the order of grating (m) and multilayer Bragg reflection order (n).

It is useful to consider the ramifications of the relationship given in Eq. 3 and Eq. 9. First, for multilayer gratings higher multilayer Bragg order contamination of the dispersed beam is eliminated since only the wavelengths strongly diffracted by the multilayer are dispersed by the grating. These are separated since the dispersion angle ϕ_m is inversely proportional to n, the multilayer Bragg order.

Second, the spectral range dispersed in any grating order is determined by the bandpass of the multilayer Bragg diffraction peak. This is always (8) less than10%, so that interference between orders does not occur until very high order. Thus, very high resolutions are obtainable in higher order.

Third, the dispersion angle ϕ is independent of λ and θ. This has specific ramifications for both true laminar phase gratings (7) and blaze gratings (7). If the step height in a true larninar phase grating is matched to the multilayer period (d_0) and the grating period (d_g) as defined by Equations 9 it will be on phase for all angles of incidence and thus for all Bragg diffracted wavelengths. Also, if the blaze angle of a blaze grating is an integral multiple of the dispersion angle ϕ as defined in Eq. 9 it will be on blaze at all angles of incidence and thus for all Bragg diffracted wavelengths. This greatly extends the useful spectral ranges of these two optic structures and is a unique property of multilayer gratings. As a result of the limited spectral range of the multilayer Bragg diffraction peaks, these optics may be used in high order so that very high resolutions are attainable.

The fact that ϕ_m is constant and independent of θ and hence λ allows very simple multilayer grating monochromators to be designed. These monochromators are directly analagous to two crystal monochromators used at XR energies. If a multilayer grating is mounted as the second element in a monochromator as shown schematically in Figure 2 and rocked off the Bragg angle by an angle $\pm$ mϕ/2 the $\pm$ m order of the grating is transported through the optic system to the detector. The monochromator may then be scanned in a manner directly analagous to XR two crystal monochromators. In the case of laminar phase gratings or blaze gratings the rocking angle will be either $\pm$ mϕ/2 or the blaze angle respectively. As multilayers are in depth diffraction reflectors there will be additional interference of light reflected at different depths in adjacent grating surfaces. This will allow rocking off the angles given above to other laminar or blaze orders eliminating contamination by specularly reflected light, particularly for the multilayer blaze grating.

In summary, multilayer gratings (amplitude, laminar phase, blaze) have properties that greatly extend their utility and have the potential for very high resolution in high order. These characteristics are not limited to the XR, SXR and EUV but will also be present with more traditional gratings intended for use at lower energies. The characteristics described here are therefore general in nature and represent a new class of optic structure.

EXPERIMENTAL RESULTS

The experimentally observed properties of multilayer diffraction gratings are presented here. Results demonstrating that Eq. 9 describes the scalar properties of these gratings is given first. Second, measured efficiencies and resolutions are reported and compared to estimates for the monochromator-source system used. Third, application of these gratings in a two element monochromator arrangement is demonstrated. Fourth, experimental results demonstrating that these multilayer diffraction gratings behave as "x-ray prisms" are presented.

Experimental results for a multilayer grating having a period of 2000 nm coated with a rhodium/carbon {t(Rh) = t(C)} multilayer having a period of 8.0 nm and containing 40 periods are described first. The grating was mounted as the second element in the two element monochromator described earlier. The disperson angle ϕ was measured both by rocking the grating holding the detector fixed and by vertically scanning the detector holding the grating fixed.

Detector scan data is shown in Figure 3 with the intensity in the m = 0, $\pm$1 orders. Note that the bandpass of this multilayer is ~ 5% so the the intensities are in a 6 eV wide energy band. Also shown in Figure 3 is a comparison of the uncorrected dispersion angle, ϕ_0, and the observed dispersion angle ϕ. At this energy (~110 eV) the refraction correction is substantial (9%). Note, more than $\pm$ 15 grating orders were observed in the grating rock mode. Scans of light dispersed by gratings coated with non-symmetric multilayers ($t_A \neq t_B$) for which higher multilayer Bragg orders are observed

showed these orders are separated in agreement with Eqs. 3, 6 and 9.

Φ was measured for 5 deg $\leq \theta \leq$ 55 deg (1006 eV $\geq E \geq$ 104 eV) and is listed in Table I. The ratio ϕ/ϕ_0 (ϕ_0 = 0.458 deg) is also shown and is seen to vary by approximately 5% over the full energy range studied, except in the region of the carbon K absorption edge at 283 eV in agreement with Eq. 9. $\bar{\delta}$ (see Eq. 8) for the rhodium-carbon multilayer structure was derived from these data (9) using Eq. 9, given d_0, d_g, m, n, and θ, and in Figure 4 is compared to values calculated using Equation 8 and the optical constants tabulated by Henke et al(10). Agreement is good at energies less than the carbon K edge (~283 eV) while at the higher energies (600 to 1000 eV) it is moderately good. The distinct minima in the calculated value of $\bar{\delta}$ at approximately 400 eV results from the energy dependence of the optical constants of the rhodium. The sharp minima in the experimental data at the carbon K edge (~283 eV) results from the energy dependence of the optical constants of the carbon and is a significant result since it is believed that the refractive indices of very low Z elements are larger than unity over a limited energy range on the high energy side of their K edges. These data may be unfolded to give the energy dependence of δ for carbon in this region by using literature values for the δ of rhodium. Such analysis shows δ for carbon is negative in this energy range so that its refractive index is larger than unity.

The conclusions to be drawn from these results are that Equation 9 describes the general properties of these simple multilayer gratings. Further, the optical constants of the multilayer

structure may be easily determined by measurement of ϕ as a function of energy with a knowledge of d_0 , d_g , n, m, and θ. This may represent a transfer standard for optical constant studies as many of the limitations of traditional techniques for optical constant determination are absent. Also, it is possible to absolutely calibrate a simple multilayer identical to the multilayer on the grating as the refractive index correction may be absolutely determined using this technique. Note also, these data represent an application of the simple multilayer-multilayer grating monochromator previously described.

The resolutions and efficiencies of these multilayer gratings are of interest when instrumental applications are considered. Efficiencies were measured by comparing the performances of simple multilayer and multilayer grating monochromators. The multilayer studied was rhodium-carbon with a period of 3.94 nm ((t(Rh) ≅ t (C)) containing 141 periods deposited on a 2000 nm period grating. The efficiency data was taken at an energy of ~1550 eV (θ =6 deg) . A 5 μm beryllium filter provided a 500 eV low energy cutoff minimizing specular light contamination. Measured ratios of the intensities of the zeroeth grating order to the intensities measured for the two multilayer monochromator are given in Table II, ranging from approximately 24 to 30%. The ratio of the intensities measure in grating orders m = 0 to 7 at θ = 6.05 deg to the intensity measured for the two multilayer monochromator are given in Table III. It is clear that these efficiencies are large even in the sixth order of the multilayer grating. It is important to note that the even orders (i.e. m = 2,4,6,---) are not expected as the

grating is of the symmetric amplitude type. Their presence is not well understood at this time, but is believed due to the fact that multilayer diffraction imposes (11) a specific wavelength-phase relation on reflection and that the multilayers are in-depth reflectors (12) rather than surface reflectors.

Resolution measurements were made at the Al K edge (1559 eV) with the same rhodium-carbon multilayer grating structure used in the efficiency measurement. A 2.16 μm thick aluminum foil was used. The measured edge jumps, presented as I_0/I where I_0 is the intensity without the Al filter and I the intensity with the Al filter, are shown as a function of θ in Figure 5 for m = 0,2,4,6. The resolutions clearly increase in higher order and from the slopes of the measured edges are: m = 0, 32 eV; m = 2, 30.8eV; m = 4, 14.2eV; m = 6, 10.3eV. The calculated resolution for the two multilayer monochromator is 43eV which is comparable to the resolution measured for m = 0 (dE = 32eV). Further analysis is needed for an assessment of the observed resolutions for m = 2,4,6.

The resolution of a grating is estimated by calculating the grating dispersion D (7) given as

$$D = d\lambda/d\phi \qquad (10)$$

It is possible to show by differentiation of Eq.1 and use of the refraction corrected Bragg's equation that the dispersion of a multilayer grating is given by

$$D = d\lambda/d\phi = \lambda [\, \mathrm{Cos}\phi/\mathrm{Sin}\phi] \qquad (11)$$

Upon rearrangement the resolution is given by

$$E/dE = \lambda/d\lambda = Tan\phi/d\phi \qquad (12)$$

This is analagous (6) in form to the resolution of a crystalline dispersion element such as single crystal silicon obtained by differentiation of Bragg's equation. For crystalline dispersion elements the Bragg angle θ replaces ϕ and the full width half maximum of the Bragg peak replaces $d\phi$. It is clear that the multilayer grating acts as a "crystal" with a "Bragg angle ϕ" and full width half maximum $d\phi$ defined by the detector slit width and system geometry. Note that since ϕ and $d\phi$ are essentially constant, multilayer gratings are constant resolution dispersion elements just as are silicon crystals for a given Bragg order.

The expected resolution for this multilayer grating monochromator may be easily estimated assuming an incident plane wave (i.e. ignoring source size) using Eq. 12. The magnitude of $d\phi$ is determined by the detector slit width (100μm) and the grating to slit spacing (1124mm): $d\phi$ is equal to 8.9×10^{-5} rads. The refraction correction term of Eq. 9 is 0.9544 so that $Tan\ \phi_1 = 3.742 \times 10^{-3}$. Resolutions calculated using these values of $d\phi$ and $Tan\ \phi_1$ are given in Table IV and compared to the experimentally observed values. The agreement is reasonable considering the simple approximations used and the possible effects of source size.

Three important points concerning grating efficiency and resolution have been illustrated. First, the gratings have excellent

efficiency relative to simple identical multilayers. Second, multilayer gratings act as crystals relative to their resolutions. Third, these gratings may be used in high order since the spectral range dispersed is defined by the multilayer bandpass and order interferences do not occur until very high orders are reached (~m = 15 for this multilayer grating).

The mass absorption coefficient of an amorphous carbon film 0.236 μm thick (46.83 $\mu g/m^2$) was determined using two multilayer gratings in the multilayer-multilayer grating monochromator. Multilayer one was 304 stainless steel and silicon [t(Si) = 1.5 t(304SS)] with a period of 5.5 nm and contained 50 periods, and was used for 180 eV < E < 1100 eV. An 8.0 nm period rhodium-carbon [t(Rh) = t(C)] containing 40 periods was used for 90 eV < E < 210 eV. Both grating periods were 2000 nm. The measured mass absorption coefficient is shown in Figure 6 and compared to data (10,13) from the literature. Calculated resolutions for m = ±1 were for 55 for the 304 SS/Si and 86 for the Rh/C gratings. The agreement shown is good even though the data is only believed accurate to 10%. Also, fine structure at the carbon edge is not observed as a result of the low resolutions.

Another important chracteristic (14) of multilayer diffraction gratings is demonstrated by measurements of the aluminum K edge at 1558 eV using a single multilayer grating mounted in the multilayer 1 position and scanning the dispersed spectrum with a detector, θ being fixed (i.e. detector scan). This experiment was performed using four separate multilayers deposited onto simple laminar gratings (d_g = 2000 nm). The multilayers were:

Molybdenum/Silicon, d = 3.0 nm; Rhodium/Carbon, d = 3.0 nm; Tungsten/Carbon, d = 4.4 nm; Rhodium/Carbon, d = 4.0 nm. In this experiment the angular position at which 1558 eV light was dispersed was determined by measuring the angular position in 2θ of the Al K absorption edge introduced into the dispersed spectrum using a 4.25 μm thick aluminum absorber. Representative data for the 3.0 nm Molybdenum/Silicon grating at θ values of 8.05 deg (~1655 eV), 8.55 deg (~1558 eV) and 9.0 deg (~1470 eV) are shown in Figure 7. Scans both with and without the aluminum absorber are shown. The positions of the aluminum K edge is denoted by the vertical arrows on the aluminum absorber scans. A 25 μm Be filter absorber was used to give a low energy cutoff of ~800 eV for the incident beam.

The important result demonstrated in Figure 7 is that the position of the aluminum edge is to the low angle side of the Bragg peak (higher energy, m negative) of the Bragg peak for θ = 9 deg (~1470 eV), directly on the Bragg peak for θ = 8.55 deg (~1558 eV) and to the high angle side (lower energy, m positive) of the Bragg peak for θ = 8.05 deg (~1655 eV). Analysis of all data for this multilayer grating (30 detector scans) demonstrated that the angular position in 2θ of the aluminum K edge was fixed relative to the incident beam at an angle of 17.1 deg corresponding to a Bragg angle of 8.55 deg. This is just the Bragg angle observed for 1558 eV light for this multilayer. This demonstrates that multilayer gratings disperse light in a continuous manner with high energies appearing at smaller angles relative to the incident beam (small Bragg angles) and lower energies at larger angles relative to the

incident beam (larger Bragg angles). Multilayer gratings therefore act as X-RAY PRISMS, as a consequence of the convolution of the effects of the two periodic structures--i.e. the multilayer and the grating. This is an unexpected result that allows fixed angle of incidence spectrographs with resolutions and spectral ranges defined by the structural parameters of the multilayer grating and the geometry of the instrument used to be designed.

DISCUSSION

Published characterizations (15,16,17) and analysis (18) of multilayer gratings are very limited. Almost all of the work has been devoted to using multilayers to enhance the reflectivity of the active grating surfaces, thereby enhancing the efficiencies of the gratings. Use of multilayer gratings for determination of the optical constants (9) of the multilayer component materials has been reported, as has the observation that multilayer amplitude gratings act as SXR prisms (14). Rife (19) has also proposed that multilayer blaze and laminar phase gratings have the potential for achieving very high resolution in high grating orders.

The experimental results presented here have allowed definition of the unique properties of multilayer gratings in agrrement with the analytical result given in Equation 9.

Particularly important are the separation of the Bragg orders of the multilayer diffracted light by the grating and the nearly constant value of ϕ_m. the dispersion angle of the m^{th} grating order relative to zeroeth order of the grating. These two properties allow the design of potentially high resolution multilayer blaze and laminar phase gratings and extremely simple monochromators and spectrometers for the XR, SXR and EUV. Results for multilayer grating efficiency and resolution and the performance of multilayer-multilayer grating monochromator supporting these conclusions were also presented. Full attainment of this potential is dependent on an accurate knowledge of the optical constants of the multilayer materials, accurate control of the multilayer period, and multilayer composition and the availability of very high quality grating substrates.

Grating quality as defined here requires an accurate knowledge of the grating period, an accurate knowledge of the blaze angle of blaze grating substrates, or the step height of laminar phase grating substrates and surface roughnesses on the grating flats of 0.3 nm or less. These are demanding requirements. Additionally the figure of the grating must be very good.

The Raleigh criteria (7) for a multilayer grating is

$$h < d_0/4m \qquad (13)$$

where h is the deviation of a given surface from the desired figure, d_0 the multilayer period and m the grating order. This requires that the grating substrate surface not deviate from the desired figure by

more than 1.0 nm for a 4.0 nm multilayer grating for m =1. The potential for very high resolution is dependent on operation in high order so that the grating figure required will be of truly atomic dimension. It is likely that such perfection will be difficult to achieve. The Bragg diffraction charactertistics of multilayer structures relax this requirement somewhat.

At the Bragg peak a standing wave field exists in the multilayer (12) that has a period essentially equal to d_0. The phase of this standing wave field varies with incident light wavelength at fixed θ, light of a given wavelength having a specific phase. Therefore, light diffracted from different grating bars or active surfaces is in phase at those surfaces. Hence, if the grating bar surfaces shift by d_0 (without slope error) the phase conditions for constructive interference of the grating dispersed light are maintained in the far field. Hence, such grating substrate figure errors may moderately decrease the efficiency of a multilayer grating, but should not dramatically impact its resolution, if not excessively large. I also note that this in depth nature of the reflection from a Bragg diffractor such as a multilayer should result in typically forbidden grating orders being filled as observed for the even orders of these symmetric amplitude gratings.

The prism like characteristics of these multilayer gratings are believed to result from the wavelength dependence of the phase of Bragg diffracted SXR at fixed angle incidence θ. This phase relationship between light of wavelength λ diffracted from different grating bars imposes specific conditions on the scattering angle at

which constructive interference occurs. It is likely that this results in the prism like properties of the multilayer gratings.

CONCLUSIONS

It is clear that these simple multilayer gratings have unique properties, many of which may be explained by simple scalar theory. These properties allow the design of simple monochromators for XR, SXR and EUV with a clear potential for high throughput and very high resolution in high grating order.. Particularly promising are multilayer blaze and laminar phase grating structures. It is also clear that our understanding of the subtleties of these optic structures is limited, and that there is substantial opportunity for creative productive research in this exciting area.

ACKNOWLEDGMENTS

The author wishes to thank the staff of the Stanford Synchrotron Radiation Laboratory for their support during the course of this work. This research benefitted from facilities at the National Science Foundation Center for Materials Research at Stanford University. This work was performed under the auspices of the U. S. Department of Energy by Lawrence Livermore National Laboratory under Contract No. W-7405-Eng-48.

Table I

The dispersion angle ϕ of light diffracted from a mulyilayer grating (d_0 = 8.0nm, N = 40, t(Rh) = t(C), d_g = 2000 nm) is presented and compared to ϕ_0. $\bar{\delta}$(exp) derived from ϕ is compared to calculation.

Θ (deg)	E(eV)	Φ(deg)	Φ/Φ_0	$\bar{\delta}$(exp)	$\bar{\delta}$(calc)
5	1006	0.4053	0.884	8.33 x10^{-4}	1.16x10^{-3}
6	848	0.4004	0.874	1.29 x10^{-3}	1.57x10^{-3}
7	755	0.386	0.842	2.16 x10^{-3}	1.85x10^{-3}
8	603	0.426	0.929	1.45 x10^{-3}	2.3 x10^{-3}
16.3	280.8	0.4507	0.983	1.3 x10^{-3}	--
16.4	279.9	0.4494	0.980	1.54 x10^{-3}	--
16.5	281.5	0.4443	0.969	2.3 x10^{-3}	--
20.0	243.5	0.4265	0.931	7.9 x10^{-3}	7.63x10^{-3}
24.0	206	0.4233	0.924	1.23 x10^{-2}	1.13x10^{-2}
26.5	188.8	0.4217	0.920	1.54 x10^{-2}	1.36x10^{2}
41.0	130	0.4161	0.908	3.85 x10^{-2}	3.12x10^{-2}
45.0	119.4	0.4206	0.918	4.05 x10^{-2}	3.81x10^{-2}
55.0	104	0.4168	0.909	6.0 x10^{-2}	5.45x10^{-2}

Table II

Efficiency of multilayer-multilayer grating monochromator for m = 0 relative to a multilayer-multilayer monochromator as a function of θ.

θ (deg)	Efficiency (%)
5.0	30
5.5	22
5.8	26
5.9	27
6.0	24
6.05	23.5

Table III

Efficiency of a multilayer-multilayer grating monochromator in ordersm = 1,2,3,4,5,6, and 7. relative to a multilayer-multilayer monochromator for θ = 6.05 deg.

m	Efficiency (%)
0	23.5
1	16.0
2	8.4
3	5.6
4	3.7
5	2.4
6	1.6
7	1.2

Table IV

Multilayer-multilayer grating monochromator resolutions for m= 0, 2, 4 , 6determined from measurements of the Al K edge.

	Experiment		Calculation	
m	λ/dλ	dE(eV)	λ/dλ	dE(eV)
0	48	32	35.4*	43*
2	50.6	30.8	84	18.6
4	110	14.2	168	9.3
6	151	10.3	254	6.2

*Calculated values are for a two multilayer monochromator

FIGURE CAPTIONS

Figure 1. Schematic of a two multilayer dispersion element vacuum monochromator.

Figure 2. Schematic drawing of an amplitude multilayer diffraction grating.

Figure 3. Grating dispersed light distribution measured by detector scan.

Figure 4. Experimental values of δ for a rhodium-carbon multilayer (d_0 = 8.0 nm, N = 40, [t(Rh) = t(C)] on a 2000 nm grating, are compared to values calculated from the compilation of Henke, et. al. (10).

Figure 5. Measurements of the aluminum K edge at 1558.98 eV made using a multilayer-multilayer grating monochromator in grating orders m = 0, 2, 4, and 6, are shown as a function of θ.

Figure 6. The mass absorption coefficient (μ/ρ) of amorphous carbon measured using a multilayer-multilayer grating monochromator in first order is shown.

Figure 7. Grating dispersed light observed as a function of detector position at fixed angles of incidence θ (8.05 deg, 8.55 deg, 9.0 deg) of a white x-ray beam (800 to 3000 eV) onto a multilayer grating with and without a 4.25 μm thick aluminum absorber in the beam. Note the position of the Al K edge as indicated (↑).

REFERENCES

1. M. Born and E. Wolf, Principles of Optics. Pergamon Press, New York (1983).

2. T. W. Barbee, Jr., Opt. Eng. 25, 989 (1986).

3. T. W. Barbee, Jr. in Low Energy X-Ray Diagnostics -1981 D. T. Attwood and B. L. Henke, eds., AIP Conf. Proc. No 75, AIP, New York (1981), P. 131

4. D. Ciarlo and D.E. Miller, in Multilayer Structures and Laboratory X-Ray Laser Research, N. M. Ceglio and P. Dhez, eds., SPIE Proc. 688, SPIE, Bellingham, Wash.(1986) P. 163.

5. W. K. Warburton, Nucl. Instrum. Methods 172 ,387 (1980).

6. R. W. James, The Optical Principles of the Diffraction of X-Rays, Oxbow Press, Woodbridge, Conn. (1982)

7. M. C. Hutley, Diffraction Gratings , Academic Press, New York (1982)

8. J. H. Underwood and T. W. Barbee, Jr., in Low Energy X-ray Diagnostics-1981, D. T. Attwood ad B. L. Henke, eds., AIP Conf. Proc. No. 75, AIP, New York (1981), P. 170

9. T. W. Barbee, Jr., in X-ray and Vacuum Ultraviolet Interaction Data Bases, Calculations and Measurements, N. delGrande and D. Y. Smith, eds.,SPIE Proc. 911, SPIE, Bellingham, Wash. (1988) P. 169

10. B. L. Henke, P. Lee, T. J. Tanka, R. L. Simabukuro, and B. K. Fujikawa,Atomic and Nuclear Data Table 27 , Academic Press, New York (1982)

11. This is treated in Ref. 1 in detail. The wavelength dependence of the phase change on diffraction by a multilayer is usually ignoredbut is important for multilayer gratings.

12. T. W. Barbee, Jr. and W. K. Warburton, Materials Letters 3 , 17(1984)

13. D. Denley, P. Perfetti, R. S. Williams, and D. A. Shirley, Pys. Rev B 21, 2267(1980)

14. T. W. Barbee, Jr., in Multilayers: Synthesis, Properties and Non-Electronic Applications, T. W. Barbee, Jr., F. Spaepen and L. Greer, eds., MRS SympVol. 103, MRS, Pittsburgh (1988) P. 307

15. R. A. M. Keski-Kuha, Applied Optics 23 , 3534 (1984)

16. W. Jark, Optics Communications 65 , 202 (1986)

17. A M Hawryluk, N. M. Ceglio, D. G. Stearns, K. Danzman, M. Kuhne, P. Muller and B. Wende, in Multilayer Structures and Laboratory X-ray Laser Research, N. M. Ceglio and P. Dhez, eds., SPIE Proc. 688, SPIE,Bellingham, Wash. (1987) P. 81

18. B. Vidal, P. Vincent, P. Dhez and M. Neviere in Applications of Thin-film Multilayer Structures to X-ray Optics, G. F. Marshall, ed., SPIE Proc. 563, SPIE, Bellingham, Wash. (1985) P. 142

19. J. Rife, Private Communication

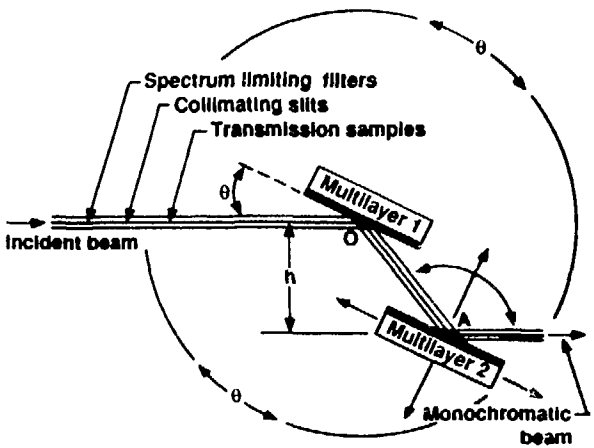

BARBEE
Figure 1

Multilayer grating

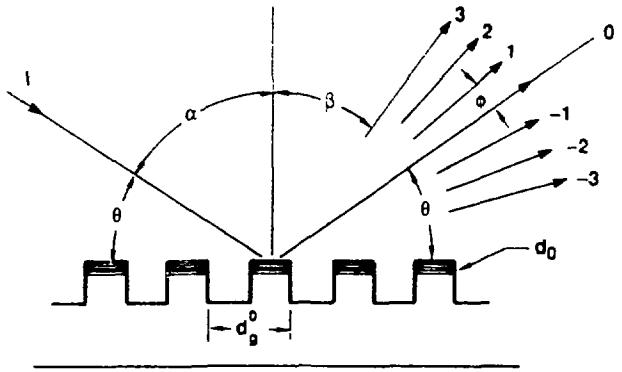

θ — Bragg angle
0 — Bragg diffracted beam
±1, ±2, ±3 — Grating dispersed Bragg light

Variables — θ, d_0, d_g^0, α, β, φ

Barbee
Figure 2

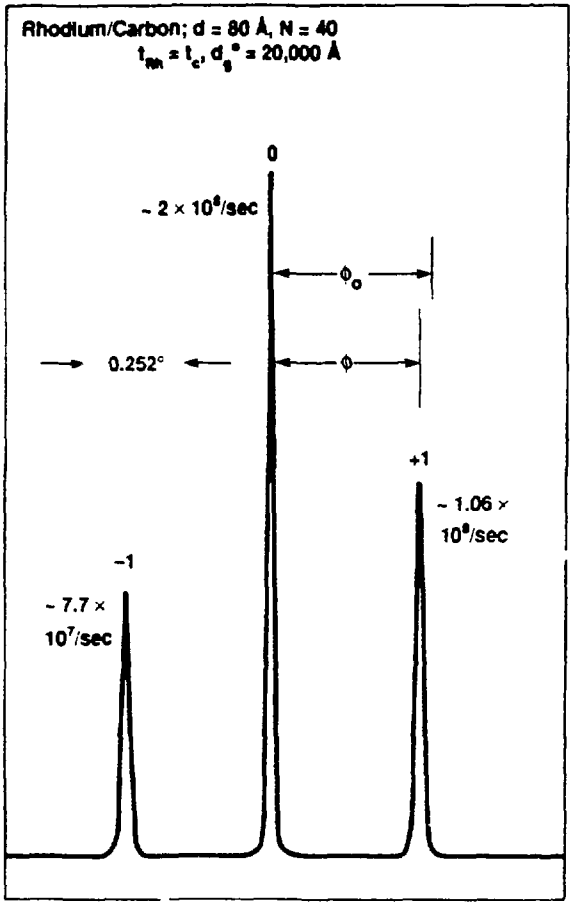

BARBEE

Figure 3

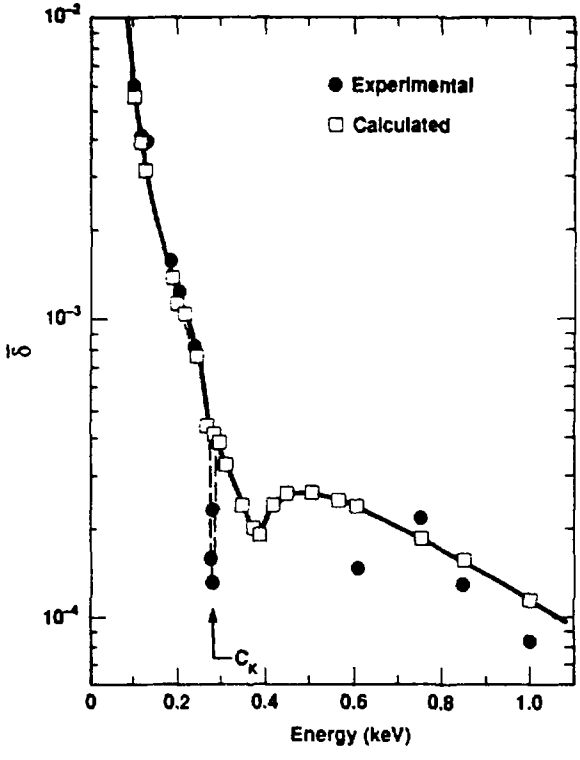

BARBEE

Figure 4

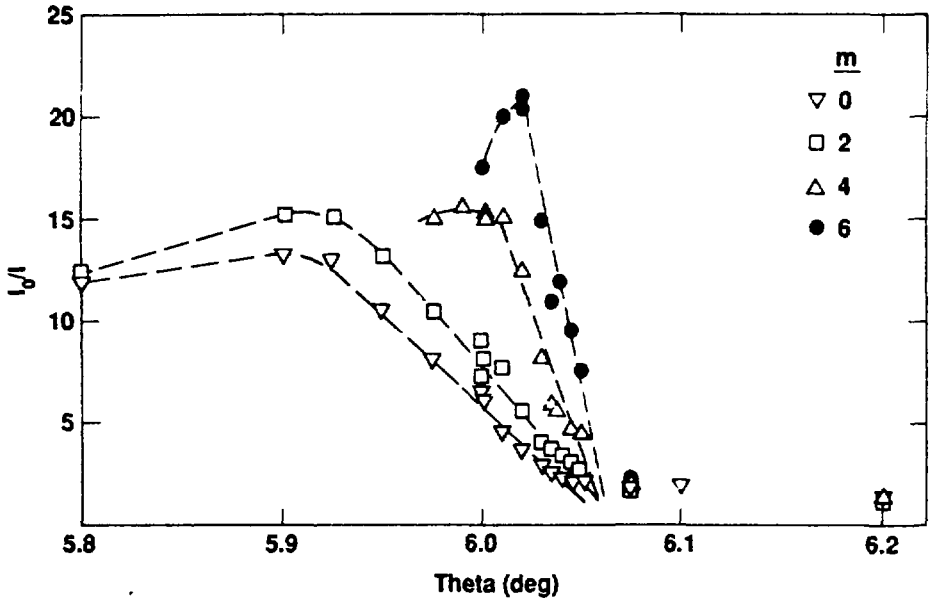

BARBEE

Figure 5

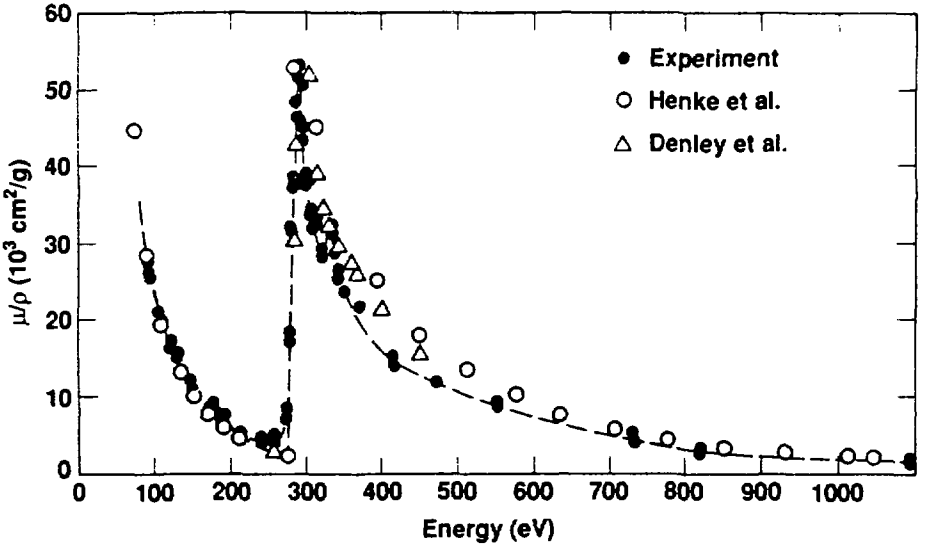

BARBEE

Figure 6

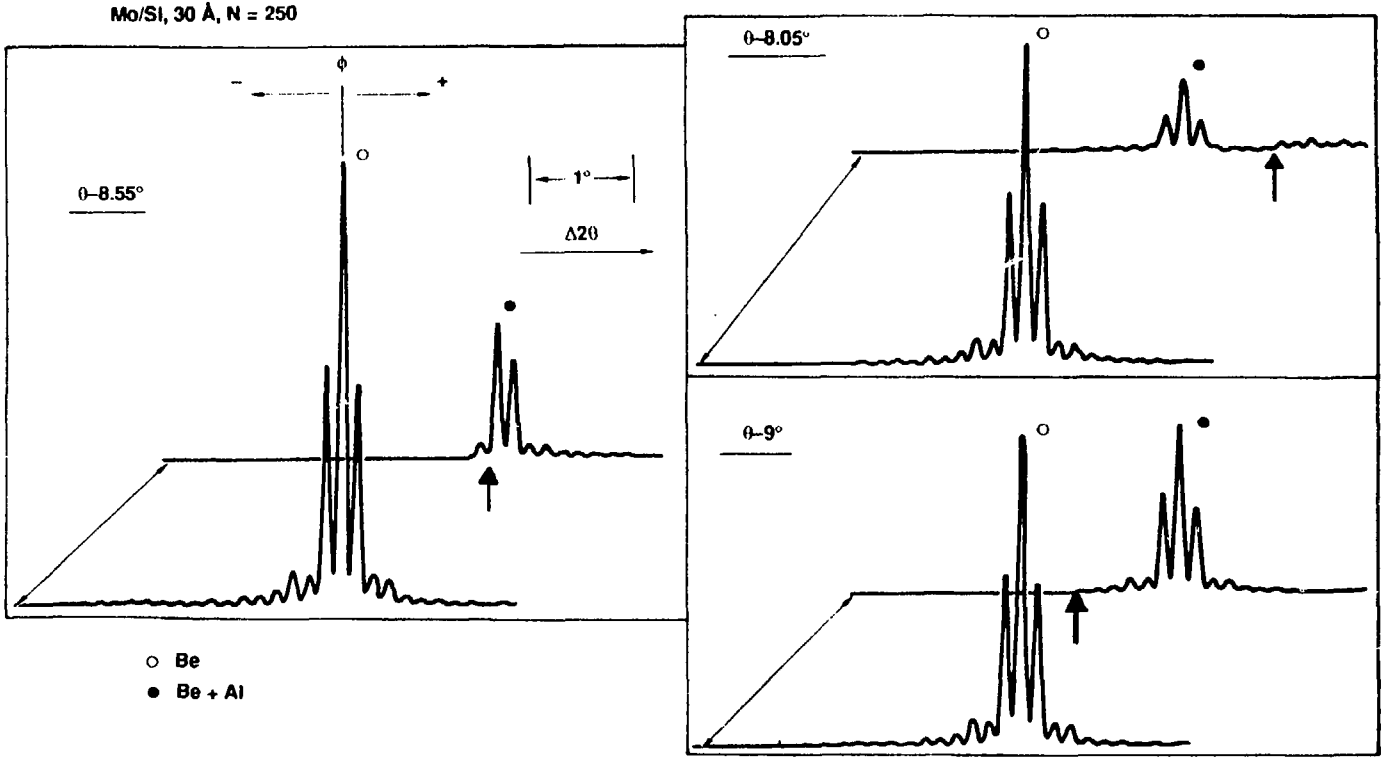

BARBEE

Figure 7